



Polarimetric Two-Scale Model for Rough Surface Bistatic Scattering Evaluation

Gerardo Di Martino, Alessio Di Simone, Antonio Iodice, and Daniele Riccio
Università di Napoli Federico II, Napoli, Italy

Abstract

The Two-Scale Model (TSM) is a widely used approach for the computation of scattering from rough surfaces. However, in its original formulation a computationally intensive numerical integration is required to effectively model depolarization effects. In the last decade the Polarimetric TSM (PTSM) has been developed to overcome this limitation, providing a closed-form expression able to account cross-polarization and depolarization effects. Very recently, PTSM has been also extended to the case of anisotropic rough surfaces (A-PTSM). However, until now only the monostatic configuration has been considered. In this paper we extend A-PTSM to the general case of bistatic scattering, presenting the procedure to obtain all the elements of the bistatic polarimetric covariance matrix. Finally, the behavior of the obtained elements is discussed and relevant numerical examples are provided and compared to more refined, but more computationally intensive, methods.

1 Introduction

The Two-Scale Model (TSM) is a method, introduced about fifty years ago [1-2], for the evaluation of scattering from rough surfaces [1], with an emphasis on sea surfaces [2]. Within its framework the rough surface results from the combination of two different roughness regimes according to the considered horizontal scale: a large-scale roughness, with horizontal scale very large with respect to the wavelength and vertical deviations of the order of the wavelength or higher, and a small-scale roughness, with horizontal scale of the order of the wavelength and vertical deviations much smaller than the wavelength. Thanks to this representation the Small Perturbation Method (SPM) [3] can be conveniently used to compute scattering from small-scale roughness, whereas Geometrical Optics (GO) [3] can be employed to evaluate scattering from large-scale roughness. Accordingly, the field scattered from small-scale roughness will be mainly dependent on small-scale roughness spectrum and will be dominant in far-from-specular directions, whereas the field due to large-scale roughness will mainly depend on large-scale roughness root mean square (rms) slopes and will be dominant in near-specular directions.

Thanks to the TSM, the monostatic co-polarized normalized radar cross section (NRCS) can be evaluated, with a high computational efficiency, simply combining the analytical closed form expressions of GO and SPM.

However, in order to take into account the cross-polarization and de-polarization effects, which need to be included in the context of a fully polarimetric analysis, the SPM expression of scattering from small-scale roughness must be averaged over the surface slopes of the large-scale roughness. In the standard TSM this average operation is obtained via numerical integration, thus dramatically reducing the computation efficiency. The problem of finding an approximated closed-form TSM expression, was considered in [4] for the backscattering configuration, leading to the development of the fully polarimetric version of TSM was named Polarimetric TSM (PTSM), which has been used in support of soil moisture retrieval from polarimetric Synthetic Aperture Radar (SAR) data [4-6]. More recently, the PTSM, which was originally applied to statistically isotropic rough surfaces, was extended to the case of anisotropic surfaces (A-PTSM), and conveniently used for the computation of backscattering from sea surfaces [7-8]. First examples of the extension of the PTSM to bistatic scattering from isotropic rough surfaces has been outlined in [8]. In this paper we extend A-PTSM to the general case of bistatic scattering from anisotropic rough surfaces.

The work is organized as follows. In Section 2, we present the procedure to obtain all the elements of the bistatic polarimetric covariance matrix in closed form. In Section 3 we present numerical results relevant to the diagonal terms of the bistatic covariance matrix in linear polarization. Finally, in Section 4 some concluding remarks are provided.

2 Bistatic Anisotropic PTSM Formulation

According to our TSM approach, the scattering surface is modeled as a collection of randomly rough (small-scale roughness) facets, randomly tilted according to the slope of the large-scale roughness. The contribution from the large-scale roughness is computed via the GO, whose corresponding closed-form expressions for the elements of the covariance matrix are available in literature, e.g. in [3]. To evaluate the contribution from the small-scale roughness, the covariance scattering matrix of a tilted rough facet is computed by using the SPM. The covariance scattering matrix of the overall surface is then obtained by averaging the one of the tilted facet with respect to facet random slopes.

In order to implement the model the power spectral density (PSD) of the small-scale roughness $W(\kappa, \varphi)$, which is a function of the amplitude of the surface wavenumber vector, κ , and of the angle between the

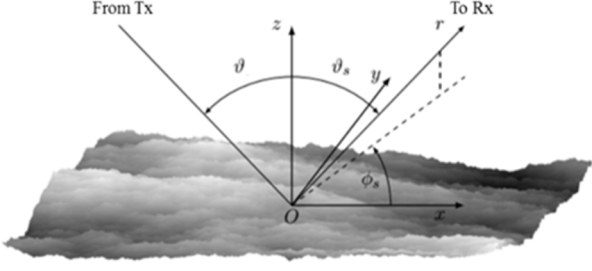


Figure 1. Geometry of the problem and coordinate system

surface wavenumber vector and the x axis, φ , (see Fig. 1), must be assigned. Moreover, the probability density function (pdf) of the large-scale roughness slopes must be specified: a usual assumption is that surface slopes along x and y directions, s_x and s_y , are zero-mean jointly Gaussian random variables with variances σ_x^2 , σ_y^2 , respectively, and correlation coefficient ρ .

According to the SPM the bistatic covariance matrix elements of the tilted facet can be expressed in the facet local reference system, i.e., in terms of the local incidence ϑ_{li} and scattering ϑ_{ls} , φ_{ls} angles, and rotation angles β_i and β_s of incidence and scattering planes, as:

$$R_{pq,rs}^{SPM} = \frac{4}{\pi} k^4 \cos^2 \vartheta_{li} \cos^2 \vartheta_{ls} \chi_{pq} \chi_{rs}^* W(\bar{\kappa}_i, \bar{\varphi}_i) \quad (1)$$

where the subscripts p, q, r, s may each stand for h (horizontal polarization) or v (vertical polarization), so that $R_{pq,pq}$ is the NRCS σ_{pq}^0 at pq polarization. In addition, k is electromagnetic wavenumber, $\bar{\kappa}_i = \sqrt{\kappa_{lx}^2 + \kappa_{ly}^2}$ and $\bar{\varphi}_i = \arctan(\kappa_{ly}/\kappa_{lx})$, with

$$\begin{aligned} \kappa_{ly} &= -k \sin \vartheta_{ls} \sin \varphi_{ls} \\ \kappa_{lx} &= -k \sin \vartheta_{ls} \cos \varphi_{ls} + k \sin \vartheta_{li} \end{aligned} \quad (2)$$

Finally,

$$\underline{\underline{\chi}}(\vartheta_{li}, \vartheta_{ls}, \varphi_{ls}, \beta_i, \beta_s) = \underline{\underline{R}}_2(\beta_s) \cdot \begin{pmatrix} F_{hh} & F_{hv} \\ F_{vh} & F_{vv} \end{pmatrix} \cdot \underline{\underline{R}}_2^{-1}(\beta_i) \quad (3)$$

where $\underline{\underline{R}}_2(\beta_{i,s})$ is the 2x2 rotation matrix, accounting for the rotation of the local polarization incidence and scattering planes with respect to the global ones, and $F_{pq}(\vartheta_{li}, \vartheta_{ls}, \varphi_{ls})$ are the bistatic Bragg coefficients [3].

Then, the local incidence ϑ_{li} and scattering ϑ_{ls} , φ_{ls} angles, and rotation angles β_i and β_s of incidence and scattering planes, must be expressed in terms of global incidence ϑ_i and scattering ϑ_s , φ_s angles and of local surface slopes s_x and s_y ; expressions for ϑ_{li} and β_i are already available in literature, see [7, eq.(23)]. The final expression of the other ones is reported here:

$$\cos \vartheta_{ls} = \frac{-s_y \sin \vartheta_s \sin \varphi_s - s_x \sin \vartheta_s \cos \varphi_s + \cos \vartheta_s}{\sqrt{1 + s_x^2 + s_y^2}} \quad (4)$$

$$\cos \varphi_{ls} = \frac{1}{\sqrt{(\sin \vartheta_i - s_x \cos \vartheta_i)^2 + s_y^2}}$$

$$\begin{aligned} & \left(\frac{(\sin \vartheta_i - s_x \cos \vartheta_i)(\sin \vartheta_s \cos \varphi_s + s_x \cos \vartheta_s)}{\sqrt{(\sin \vartheta_s \cos \varphi_s + s_x \cos \vartheta_s)^2 + (-s_y \cos \vartheta_s - \sin \vartheta_s \sin \varphi_s)^2 + (-s_x \sin \vartheta_s \sin \varphi_s + s_y \sin \vartheta_s \cos \varphi_s)^2}} + \right. \\ & \left. + \frac{s_y \cos \vartheta_i (-s_y \cos \vartheta_s - \sin \vartheta_s \sin \varphi_s) + s_x \sin \vartheta_i (-s_x \sin \vartheta_s \sin \varphi_s + s_y \sin \vartheta_s \cos \varphi_s)}{\sqrt{(\sin \vartheta_s \cos \varphi_s + s_x \cos \vartheta_s)^2 + (-s_y \cos \vartheta_s - \sin \vartheta_s \sin \varphi_s)^2 + (-s_x \sin \vartheta_s \sin \varphi_s + s_y \sin \vartheta_s \cos \varphi_s)^2}} \right) \end{aligned} \quad (5)$$

$$\tan \beta_s = \frac{s_x \sin \varphi_s - s_y \cos \varphi_s}{s_y \cos \vartheta_s \sin \varphi_s + s_x \cos \vartheta_s \cos \varphi_s + \sin \vartheta_s} \quad (6)$$

Full derivation of (4-6) will be provided in [9].

At this point, we proceed expanding the bistatic covariance matrix elements of the tilted facet, (1), in power series of facet slopes s_x and s_y and arresting the expansion at the second order, thus obtaining:

$$\begin{aligned} R_{pq,rs}^{SPM}(\vartheta_{li}, \vartheta_{ls}, \varphi_{ls}, \beta_i, \beta_s) &\cong \frac{4}{\pi} k^4 \cos^2 \vartheta_{li} \cos^2 \vartheta_{ls} F_{pq} F_{rs}^* W(\bar{\kappa}, \bar{\varphi}) + \\ &+ D_{1,0}^{pq,rs} s_x + D_{0,1}^{pq,rs} s_y + D_{2,0}^{pq,rs} s_x^2 + D_{0,2}^{pq,rs} s_y^2 + D_{1,1}^{pq,rs} s_x s_y \end{aligned} \quad (7)$$

where

$$D_{k,n-k}^{pq,rs} = \frac{1}{n!} \binom{n}{k} \frac{\partial^n R_{pq,rs}^{SPM}}{\partial s_x^k \partial s_y^{n-k}} \Big|_{s_x=s_y=0}, \quad (8)$$

$\bar{\kappa} = \sqrt{\kappa_x^2 + \kappa_y^2}$ and $\bar{\varphi} = \arctan(\kappa_y/\kappa_x)$, with

$$\begin{aligned} \kappa_y &= -k \sin \vartheta_s \sin \varphi_s \\ \kappa_x &= -k \sin \vartheta_s \cos \varphi_s + k \sin \vartheta_i, \end{aligned} \quad (9)$$

and F_{pq} are evaluated in $\vartheta_i, \vartheta_s, \varphi_s$.

The derivatives in (8) can be analytically computed in closed form, although their expressions are rather involved and will be reported elsewhere [9].

Finally, bistatic covariance matrix elements of the overall surface can be obtained by averaging with respect to facet slopes:

$$\begin{aligned} \langle R_{pq,rs}^{SPM}(\vartheta_{li}, \vartheta_{ls}, \varphi_{ls}, \beta_i, \beta_s) \rangle &\cong \frac{4}{\pi} k^4 \cos^2 \vartheta_{li} \cos^2 \vartheta_{ls} F_{pq} F_{rs}^* W(\bar{\kappa}, \bar{\varphi}) + \\ &+ D_{2,0}^{pq,rs} \sigma_x^2 + D_{0,2}^{pq,rs} \sigma_y^2 + D_{1,1}^{pq,rs} \rho \sigma_x \sigma_y \end{aligned} \quad (10)$$

3 Numerical Results

We here present some numerical results relative to the bistatic linear-polarization NRCS. We focus on the case

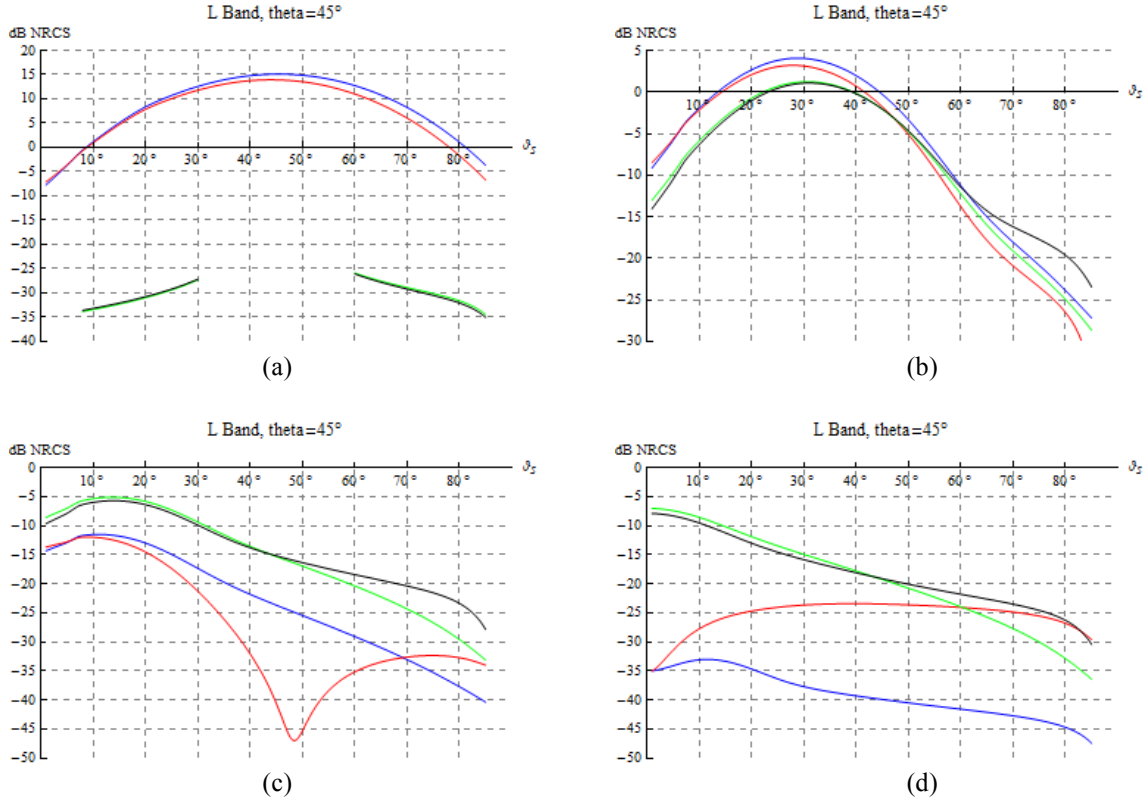


Figure 2. VV (red), HH (blue), HV (green), and VH (black) NRCS vs. the scattering angle ϑ_s at L band (frequency = 1.58 GHz, $\epsilon = 75-j61$), $\vartheta_i = 45^\circ$, and $u_{10} = 10$ m/s, upwind, for $\varphi_s = 0^\circ$ (a), $\varphi_s = 30^\circ$ (b), $\varphi_s = 60^\circ$ (c), $\varphi_s = 90^\circ$ (d).

of the sea surface, so that for the PSD of the small-scale roughness we use the high-frequency part of the Elfouhaily spectrum [10] and, regarding the large-scale roughness, we evaluate σ_x^2 , σ_y^2 , and ρ using the approach presented in [7]. Accordingly, all these parameters can be evaluated as functions of the speed and direction of the wind.

In Fig.2 we show the linear-polarization NRCSs at L band, upwind (wind blowing along the direction of the x axis), wind speed 10 m/s, at 45° incidence angle as functions of the scattering angle for four different azimuth scattering angles. Regarding the graphs of Fig.2(a), i.e. for $\varphi_s = 0^\circ$, it is important to note that the GO contribution for the HV and VH NRCSs is equal to 0, so that it cannot be used to evaluate the scattering in near-specular directions (around $\vartheta_s = 45^\circ$), where the SPM does not hold. For this reason, the A-PTSM cannot be used to compute these NRCS in the vicinity of $\vartheta_s = 45^\circ$. However, it is meaningful to highlight that for $\varphi_s = 0^\circ$ these cross-polarized NRCSs would be 0 for any incident and scattering angle according to SPM, if random tilt of the facets is not introduced.

Finally, note that the presented graphs are obtained using a set of parameters that makes them directly comparable with those of [11, Fig.6], obtained via the second order small slope approximation (SSA2). It can be verified that our results are in good agreement with those of the more refined SSA2, although the latter requires computationally

intensive fourfold numerical integrations, whereas our formulation is in closed form.

4 Conclusion

In this work, we have discussed the extension of the A-PTSM introduced in [7] to the bistatic scattering case. The procedure to obtain closed-form expressions of all the elements of the polarimetric covariance matrix has been presented. Graphs of the NRCS diagonal terms of the bistatic polarimetric covariance matrix have been obtained, for the special meaningful case of the sea surface modeled via the directional Elfouhaily spectrum and an anisotropic jointly Gaussian distribution of surface slopes. Finally, the numerical results have been positively compared with those of other, more refined but less computationally efficient, methods, thus demonstrating the soundness of the presented approach.

5 References

1. G. R. Valenzuela, "Scattering of Electromagnetic Waves from a Tilted Slightly Rough Surface", *Radio Sci.*, **3**, pp. 1057-1066, 1968.
2. J. W. Wright, "A New Model for Sea Clutter", *IEEE Trans. Antennas Propag.*, **16**, pp. 217-223, 1968.

3. F. T. Ulaby, R. K. Moore, and A. K. Fung, *Microwave Remote Sensing*. Reading, MA: Addison-Wesley, 1982.
4. A. Iodice, A. Natale, and D. Riccio, "Retrieval of Soil Surface Parameters via a Polarimetric Two-Scale Model", *IEEE Trans. Geosc. Remote Sens.*, **49**, 7, pp. 2531-2547, July 2011.
5. A. Iodice, A. Natale, and D. Riccio, "Polarimetric two-scale model for soil moisture retrieval via dual-pol HH-VV SAR data," *IEEE J. Sel. Topics Appl. Earth Observ.*, **6**, 3, pp. 1163–1171, Jun. 2013.
6. G. Di Martino, A. Iodice, A. Natale, D. Riccio, "Polarimetric Two-Scale Two-Component Model for the Retrieval of Soil Moisture Under Moderate Vegetation via L-Band SAR Data", *IEEE Trans. Geosc. Remote Sens.*, **54**, 4, pp. 2470-2491, 2016.
7. G. Di Martino, A. Iodice, D. Riccio, "Closed-Form Anisotropic Polarimetric Two-Scale Model for Fast Evaluation of Sea Surface Backscattering", *IEEE Trans. Geosc. Remote Sens.*, **57**, 8, pp. 6182-6194, 2019.
8. G. Di Martino, A. Di Simone, A. Iodice, D. Riccio, "Closed-form Polarimetric Two-Scale Model for sea scattering evaluation," *2019 IEEE 5th International forum on Research and Technology for Society and Industry (RTSI)*, Florence, Italy, pp. 34-38, 2019.
9. G. Di Martino, A. Di Simone, A. Iodice, D. Riccio, "Bistatic scattering from anisotropic rough surfaces via the Polarimetric Two-Scale Model", *IEEE Trans. Geosc. Remote Sens.*, to be submitted.
10. T. Elfouhaily, B. Chapron, K. Katsaros, and D. Vandemark, "A unified directional spectrum for long and short wind-driven waves," *J. Geophys. Res.*, **102**, pp. 15781–15796, 1997.
11. A. G. Voronovich and V. U. Zavorotny, "Full-polarization modeling of monostatic and bistatic radar scattering from a rough sea surface", *IEEE Trans. Antennas Propag.*, **62**, 3, pp. 1362–1371, March 2014.